

Structures and Stabilities of doubly-charged $(\text{MgO})_n\text{Mg}^{2+}$ ($n=1-29$) Cluster Ions

Francisco López, Andrés Aguado*, and José M. López

Departamento de Física Teórica, Facultad de Ciencias, Universidad de Valladolid, 47011 Valladolid, Spain

Ab initio perturbed ion plus polarization calculations are reported for doubly-charged nonstoichiometric $(\text{MgO})_n\text{Mg}^{2+}$ ($n=1-29$) cluster ions. We consider a large number of isomers with full relaxations of the geometries, and add the correlation correction to the Hartree-Fock energies for all cluster sizes. The polarization contribution is included at a semiempirical level also for all cluster sizes. Comparison is made with theoretical results for neutral $(\text{MgO})_n$ clusters and singly-charged alkali-halide cluster ions. Our method is also compared to phenomenological pair potential models in order to assess their reliability for calculations on small ionic systems. Bulk-like rocksalt structures are predominant from $n=13$ on. The relative stabilities of the cluster ions against evaporation of a MgO molecule shows variations that are in excellent agreement with the experimental abundance spectra.

PACS numbers: 36.40.c; 61.46.+w; 61.50.Lt; 61.60.+m; 79.60.Eq

I. INTRODUCTION

Cluster science has become a field of intensive research both for experimentalists and theoreticians. Small aggregates have a fundamental interest because they provide a link between the molecular and the solid state physics, and furthermore they are important in new technological applications like nanoelectronics. Elucidating the structural and electronic properties of clusters remains a major challenge for present-day science, due to the significant deviations that clusters present in their physical and chemical properties when compared both to the molecule and the bulk. Another difficulty arises from the huge increase in the number of different isomers with cluster size. Many interesting cluster properties depend largely on the cluster structure, at least in the case of ionic and covalently-bonded materials, so a complete description of the relevant isomer configurations for each cluster size is highly desirable for an appropriate understanding of cluster processes.

In the last years, considerable effort has been devoted to the understanding of metallic and semiconductor clusters. Meanwhile, studies on metal-oxide clusters have been comparatively scarce, in spite of their fundamental role in important physical processes like heterogeneous catalysis. In this work the interest is focused on magnesium oxide. Stoichiometric MgO clusters have been investigated both experimentally and theoretically. Saunders^{1,2} reported mass spectra and collision-induced-fragmentation data for sputtered $(\text{MgO})_n^+$ cluster ions, and Ziemann and Castleman^{3,4} performed experimental measurements by using laser-ionization time-of-flight mass spectrometry.^{5,6} Theoretical calculations have been performed at different levels of accuracy: simple ionic models based on phenomenological pair potentials⁷⁻⁹ were performed by Ziemann and Castleman⁴ to explain the global trends found in their experiments; semiempirical tight-binding calculations were reported by Moukouri and Noguera;^{10,11} finally, *ab initio* calculations on stoichiometric MgO clusters have been presented recently by Recio *et al.*,^{12,13} Malliavin and Coudray,¹⁴ and de la Puente *et al.*¹⁵ Nonstoichiometric $(\text{MgO})_n\text{Mg}^+$ and $(\text{MgO})_n\text{Mg}^{2+}$ cluster ions have been

also detected and studied experimentally by Ziemann and Castleman.^{3,4,16} Specifically, they have obtained, by changing the flow rate of the carrier gas in a gas aggregation source, a mass spectrum comprised almost entirely of doubly-charged $(\text{MgO})_n\text{Mg}^{2+}$ cluster ions.¹⁶ Enhanced stabilities in the small-size regime were found for $n=8,11,13,16,19,22,25,27$, and were explained in terms of compact cubic clusters resembling pieces of the MgO crystal lattice. If we exclude the pair potential calculations performed by Ziemann and Castleman,^{4,16} there is no theoretical investigation of nonstoichiometric MgO cluster ions.

The “extra” cation present in nonstoichiometric cluster ions is expected to result in large structural distortions whenever a specially compact structure can not be constructed. That is not a problem in pair potential calculations, where the simplicity of the interactions allows for a complete geometrical relaxation of the different isomers at a very modest computational cost. Nevertheless, the need to use some selected set of empirical parameters for Mg^{q+} and O^{q-} ($q=1,2$) ions results in a serious questioning of the reliability of these simple ionic models. On the opposite side, traditional *ab initio* calculations based on the molecular orbital-linear combination of atomic orbitals (MO-LCAO) approximation are very reliable but computationally expensive, the computer time requirements scaling with the fourth power of the number of atoms in the cluster. Thus, the calculations of Recio *et al.* on $(\text{MgO})_n$ and $(\text{MgO})_n^+$ clusters^{12,13} were performed under certain restrictions: (a) the geometries of most of the isomers were optimized with respect to a single parameter, namely the nearest-neighbor distance; (b) only 2 or 3 different isomers were considered for each cluster size; (c) the correlation energy corrections (calculated at the MP2 level) were included only for $n \leq 6$. In the calculations of Malliavin and Coudray¹⁴ the geometries were more carefully optimized but the results were limited to the size range $n=1-6$.

In the present work we report the results of an extensive and systematic study of $(\text{MgO})_n\text{Mg}^{2+}$ cluster ions with n up to 29. We have employed the *ab initio* perturbed ion (aiPI) model,¹⁷ which is a Hartree-Fock model based on the theory of electronic separability^{18,19} (TES)

and the *ab initio* model potential approach of Huzinaga *et al.*,²⁰ supplemented with some interaction energy terms to account for polarization contributions (see next section). The model has been successfully employed by our group in several studies of alkali halide clusters and cluster ions.^{21–25} It has been used also in a study of neutral stoichiometric $(\text{MgO})_n$ ($n=1–13$) clusters.¹⁵ On one hand, our calculations represent a major advance with respect to pair potential methods, and on the other hand, they overcome most of the technical difficulties found in more sophisticated *ab initio* methods: (a) we have allowed for an appropriate geometrical relaxation of the isomers; (b) we have studied a large set of isomers for each cluster size (specifically, the total number of isomers studied is around 400); (c) correlation corrections, which have been proved to be essential for an accurate description of metal-oxide clusters,¹⁵ have been included for all cluster sizes; (d) we have been able to study relatively large cluster sizes (up to $n=29$), enlarging thus the usual size range covered by traditional *ab initio* methods.

The structural results presented in this work could also be useful in the interpretation of possible future experimental investigations on these clusters. By measuring the mobility of cluster ions through an inert buffer gas under the influence of a weak electric field, drift tube experimental studies provide valuable information about the cluster geometries.^{27–29}

The rest of the paper is organized as follows: in section II we give a brief resume of the aiPI model as applied to clusters (full expositions of the method have been given elsewhere^{21,22}), a comparison with pair potential models which serves to assert the quality of the aiPI methodology, and the details of the computational procedure. The results are presented in section III, and finally section IV summarizes the main conclusions extracted from this study.

II. THE AIPI MODEL. COMPARISON TO PAIR POTENTIAL MODELS.

The *ab initio* perturbed ion model¹⁷ was originally designed for the description of ionic solids,³⁰ and subsequently adapted to the study of clusters in our group.^{21–25} Its theoretical foundation lies in the theory of electronic separability,^{31,32} and its practical implementation in the Hartree-Fock (HF) version of the TES.^{18,19} The HF equations of the cluster are solved stepwise, by breaking the cluster wave function into local group functions (ionic in nature in our case). In each iteration, the total energy is minimized with respect to variations of the electron density localized in a given ion. The electron densities of the other ions are frozen. In the subsequent iterations each frozen ion assumes the role of non-frozen ion. When the self-consistent process (see more details below) finishes, the outputs are the total cluster energy E_{clus} and a set of localized wave functions for each geometrically nonequivalent ion in the cluster. The cluster energy can be written as a sum of ionic additive energies:^{21–23}

$$E_{clus} = \sum_{R=1}^N E_{add}^R, \quad (1)$$

where the sum runs over all ions in the cluster, and the contribution of each particular ion to the total cluster energy (E_{add}^R) can be expressed in turn as a sum of intraionic (net) and interionic contributions:

$$E_{add}^R = E_{net}^R + \frac{1}{2} \sum_{S(\neq R)} E_{int}^{RS} = E_{net}^R + \frac{1}{2} E_{int}^R. \quad (2)$$

The localized nature of the aiPI procedure has some advantages over the usual molecular orbital models. As the correlation energy correction in weakly overlapping systems is almost intraionic in nature (being therefore a sum of contributions from each ion), the localized cluster-consistent ionic wave functions may be used to attain good estimations of this correction. In this paper, the correlation energy correction is obtained through Clementi's Coulomb-Hartree-Fock method.^{33,34} Besides, it also allows the development of computationally efficient codes³⁵ which make use of the large multi-zeta basis sets of Clementi and Roetti³⁶ for the description of the ions. At this respect, our optimizations have been performed using basis sets (5s4p) for Mg^{2+} and (5s5p) for O^{2-} , respectively. Inclusion of diffuse basis functions has been checked and shown unnecessary. Another advantage coming from the localized nature of the model is the linear scaling of the computational effort with the number of atoms in the cluster. This has allowed us to study clusters with as many as 59 atoms at a reasonable computational cost.

Selfconsistency has been achieved in the following way: for a given distribution of the ions forming the cluster, we consider one of them as the active ion R (for instance, a particular oxygen anion), and solve the Self-Consistent-Field equations for anion R in the field of the remaining ions, which are considered frozen at this stage. Next, we take another oxygen anion (anion S) as the active ion and repeat the same process. If the anion S is geometrically inequivalent to anion R, the energy eigenvalues and wave functions of electrons in anions S are different from those of anions R. We continue this process in the same way until all the anions have been exhausted. The same procedure is then followed for the magnesium cations. The process just described is a PI cycle. We iterate the PI cycles until convergence in the total energy of the cluster is achieved. Note that the selfconsistent process can be accelerated if equivalences between anions or cations are imposed by fixing the symmetry of an isomer. In order to allow for completely general distortions, we have not employed that simplification in the present study. Nevertheless, equivalences in some ionic wave functions have been observed at the end of the calculations for some highly symmetrical isomers.

It is very interesting to compare any quantum model designed for the study of ionic materials with the rigid ion and polarizable ion models.^{7–9} These pair potential models are very intuitive, and include in a phenomenological way all the relevant terms in the interatomic potential energy. The quality of an *ab initio* method developed for

application on ionic materials can thus be assted by specifying in which way it improves over a pair potential description. The binding energy in a pair potential model can be expressed as $E_{bind} = \frac{1}{2} \sum_{i \neq j} V_{ij} + \sum_i E_i^S$, where V_{ij} is the potential energy between ions i and j , and E_i^S is the self-energy of the ion i measured relative to the self-energy of the isolated atom. In the rigid ion model, we have⁹

$$V_{ij}^{rigid} = \frac{q_i q_j}{r_{ij}} + A_{ij} e^{-r_{ij}/\rho}, \quad E_i^{S,rigid} = 0. \quad (3)$$

The first term is the electrostatic Coulomb energy between two point ions with charges q_i and q_j , and the second term is the short-range repulsive Born-Mayer energy reflecting the mutual repulsion due to the overlap of the wave functions of the ions. In the polarizable ion model, a polarizability α_i is assigned to each ion so that the electron shells can be polarized by the electric field created by the other ions in the cluster. Now we have⁹

$$V_{ij}^{pol} = V_{ij}^{rigid} + V_{ij}^{MD} + V_{ij}^{DD}, \quad E_i^{S,pol} = \frac{\mu_i^2}{2\alpha}. \quad (4)$$

The self-energy is now different from zero, and the interaction energy contains two new terms: a monopole-dipole and a dipole-dipole interaction term. In the Born-Mayer repulsive potential, the distance r_{ij} is replaced by an effective value r_{ij}^{eff} to take into account the deformation of the electronic shells upon cluster formation. An intermediate pair potential model exists in which the repulsive radii of ions are allowed to deform isotropically under the effects of other ions in the system, but ionic polarizations arising from the positional displacements of each shell from its own core are not considered. This is the breathing shell model (BSM),⁴³ and constitutes an important improvement over the rigid ion model. In the aiPI model, the binding energy can be written as a sum of ionic contributions, which are in turn expressed as a sum of deformation and interaction terms²¹⁻²³

$$E_{bind} = \sum_R E_{bind}^R = \sum_R (E_{def}^R + \frac{1}{2} E_{int}^R). \quad (5)$$

The interaction energy term is of the form

$$E_{int}^R = \sum_{S \neq R} E_{int}^{RS} = \sum_{S \neq R} (E_{class}^{RS} + E_{nc}^{RS} + E_X^{RS} + E_{overlap}^{RS}), \quad (6)$$

where the different energy contributions are: the classical electrostatic interaction energy between point-like ions; the correction to this energy due to the finite extension of the ionic wave functions; the exchange interaction energy between the electrons of ion R and those of the other ions in the cluster; and the overlap repulsive energy contribution.³² The deformation energy term E_{def}^R is the self-energy of the ion R measured relative to the self-energy of the isolated ion. It is an intrinsically quantum-mechanical many-body term that accounts for the energy change associated to the compression of the ionic wave functions upon cluster formation, and incorporates the correlation contribution to the binding energy. All

those terms are calculated in an *ab initio* selfconsistent way. Thus, the improvement over the classical rigid-ion description is clear. Improvement over a polarizable-ion description can be questionable in principle due to one basic assumption used in the actual aiPI code, namely spherically symmetric electron densities, centered on the nuclei. The electron density clouds of the ions are thus allowed to distort just isotropically under the effect of the other ions in the cluster, and indeed the aiPI model could be considered as an *ab initio* breathing shell model (aiBSM). In summary, although the aiPI method treats quantum-mechanically all the terms present in a breathing shell model, plus other many-body terms absent from any classical model, it does not describe the dipolar terms present in a polarizable-ion model because there are not induced dipoles. In our previous works on alkali halide clusters,²¹⁻²⁵ inclusion of polarization was not considered essential. However, the O^{2-} anion has a very deformable density cloud (that is a large polarizability), and dipolar contributions are expected to be more important than for halide anions. Relaxing the spherical symmetry assumption would allow in principle for a proper description of those terms, but many of the computational advantages of the aiPI model (which have allowed us to perform such a detailed study) would be lost. The solution we have chosen is to include the polarization terms in the selfconsistent process with a polarizable point-ion description. In such a way, the “enlarged” aiPI model obtained improves clearly over all classical descriptions, and can be considered a benchmark for the pair potential calculations. The price to be paid is the inclusion of empirical polarizabilities for the ions. The reliability of the model is thus reduced a little compared to the most sophisticated *ab initio* methods, but complete geometrical distortions can be considered and a large number of isomers studied at less cost. Furthermore, the only cases in which doubts related to the energetical ordering of the isomers arise are those showing near-degenerate isomers, and we will show that those situations are not frequent.

Now we explain the calculational method used in our study of $(MgO)_n Mg^{2+}$ cluster ions. We had no knowledge a priori as to what shapes can adopt these clusters. So we performed an extensive sampling of the potential energy surface by generating a large set of random cluster configurations for each cluster size n with $n=1-13$. Except for the smallest sizes ($n=1,2$), typically 100,000 configurations were generated for each n . All those random configurations were fully optimized by using a rigid-ion model. The parameters in equation 3 were those used by Ziemann and Castleman,^{4,16} although some tests were also performed with the set of parameters of Bush *et al.*³⁷ Both sets of parameters led to essentially identical structures, differing just in minor details. These pair potential calculations could be performed at a low computational cost and therefore were very useful in locating reasonable initial guesses for the different minima on the potential energy surface. Then we took typically the 15-20 lowest-energy isomers obtained in the pair potential calculations for each cluster size as input geometries for the aiPI calculations. We also studied structures obtained by adding or removing in different ways a molecule from those pair-

potential structures, of course whenever such a structure was not already present in the pair-potential results. For $n=13$, a compact $3\times 3\times 3$ structure (the notation $a\times b\times c$ indicates the number of atoms along three perpendicular edges) is found to be a specially stable isomer (see next section), so for $n>13$ we have studied geometries which contain the $3\times 3\times 3$ structure as a subunit (furthermore, test pair potential and aiPI calculations performed for $n=14$ revealed that less coordinated structures are not competitive anymore from the energetic point of view). We have considered also stackings of the different planar structures found for $n\leq 13$. While we can not rule out completely the possibility of having overlooked some important isomer, we believe that we have reduced it considerably. We have performed aiPI+polarization calculations on all those isomers, without considering any equivalence between the ions. The optimizations of the geometries have been performed by using a downhill simplex algorithm.^{38,39} Bulk values have been used for the ionic polarisabilities.⁴⁰

We finish this section with a comment about the ionic character of our model. Although the aiPI model describes the MgO cluster ions in terms of Mg^{2+} and O^{2-} units, we would like to stress that it does not enter in conflict with any possible assignment of fractional charges to each ion in *classical* models. In fact, the charges used by Ziemann and Castleman^{4,16} were ± 1 , the charges in the potential of Bush *et al.*³⁷ are ± 2 , and both potentials give very similar results. The difference in the Coulomb part is compensated by a difference in the repulsive part. In other words, those charges are just parameters. On the other hand, ionic charges can be derived from quantum-mechanical calculations following the ideas of Bader.⁴¹ That has been done recently in aiPI calculations on ionic solids from which fractional ionic charges have been derived.⁴²

III. RESULTS

A. Ground State Structures and Low-lying Isomers.

In the following, we restrict our discussion to the structural properties of the lowest-lying isomers. The $(\text{MgO})_n\text{Mg}^{2+}$ aiPI+polarization structures are shown in Figure 1. The ground state (GS) and one or two low-lying isomers are given for each n , except for $n\geq 24$ where only one isomer is shown. A cutoff of 2.54 Å, that exceeds by $\approx 20\%$ the Mg–O distance in the bulk, was arbitrarily chosen in order to decide whether an O atom is bonded to a Mg neighbor or not. The energy difference with respect to the most stable isomer is given (in eV) below each isomer. For cluster sizes $n=1$ and $n=2$ (not shown in the figure), a linear chain is obtained as the GS isomer. The emergence of the bulk crystalline structure can be appreciated from fig. 1: one-dimensional chains are observed for the smallest cluster sizes ($n=1-3$); next there is a size region ($n=3-7$) where planar two-dimensional (2D) structures occur, either as the GS or as low-lying isomers; for $n=7-12$, compact three-dimensional (3D) structures are already predominant, although without a clear establish-

ment of the f.c.c. symmetry; finally from $n=13$ on, the clusters form rocksalt fragments. The $(\text{MgO})_{13}\text{Mg}^{2+}$ GS isomer is a highly compact $3\times 3\times 3$ rocksalt piece that can be considered a building block for the larger cluster sizes.

Let us describe now in more detail the structures obtained for each value of n , first for the small cluster sizes ($n<13$). Linear chains are the GS isomers for $n=1$ and $n=2$. The $n=3$ GS is a planar rectangular structure with a cation attached to a corner. A 3D structure obtained by removing an anion from a perfect cube appears just 0.04 eV above the GS, and a linear chain is still observed as a competitive isomer. The $n=4$ GS is a quasiplanar 3×3 sheet, and can be considered the first occurrence of a rocksalt fragment. A 3D isomer obtained by adding a cation to a $(\text{MgO})_4$ cubic cluster is still high in energy. Linear chains are not competitive anymore. The first 3D GS isomer occurs for $n=5$. It is a $2\times 2\times 3$ piece with an anion removed from a corner. A planar sheet obtained by adding a MgO molecule to the $n=4$ GS is obtained as a low-lying isomer. 3D structures, obtained by adding a cation to the hexagonal prism that is the GS of the neutral $(\text{MgO})_6$,¹⁵ are the lowest-lying near-degenerate isomers for $n=6$. As a low-lying isomer we find a structure that shows the $(\text{MgO})_4\text{Mg}^{2+}$ GS as a subunit. A $2\times 2\times 3$ rocksalt piece with a triatomic Mg–O–Mg attached to an edge is the GS for $n=7$. The planar sheet is found at a high energy, and 2D isomers are not competitive from this size on. A rounded cage structure with quadrangular and hexagonal faces is found as a low-lying isomer. From $n=8$ to $n=12$, signs of the emergence of the rocksalt structure are more apparent. For example, rocksalt-based structures are the GS for $n=8$ (a $2\times 3\times 3$ fragment with an anion removed from a basal plane), $n=10$ (a $2\times 3\times 3$ fragment with a triatomic Mg–O–Mg attached to an edge), and for $n=12$ (an incomplete $3\times 3\times 3$ fragment). But the establishment of f.c.c. symmetry is not complete yet. Rounded cages and structures based on stacking of hexagonal rings are obtained as low-lying isomers for these cluster sizes, and they turn out to be the GS isomers for $n=9$ and 11.

The situation changes dramatically at $n=13$. The GS isomer is a perfect $3\times 3\times 3$ rocksalt fragment, and is specially stable (the first isomer lies 5.24 eV higher in energy). This high stability makes the growing pattern simpler for the larger cluster sizes. With few exceptions, the $(\text{MgO})_n\text{Mg}^{2+}$ GS isomer ($n\geq 14$) is obtained by adding a molecule to the GS isomer of $(\text{MgO})_{n-1}\text{Mg}^{2+}$, and the establishment of the bulk structure is almost complete. The low-lying isomers are also rocksalt fragments in almost all cases. The growing pattern in this size range can also be described in terms of the stacking of an odd number of planar sheets, that are found as low-lying isomers in the size range $n=4-8$. The $n=13$ GS isomer can indeed be viewed as a stacking of three planar sheets, each one with the $(\text{MgO})_4\text{Mg}^{2+}$ GS structure. As the minimum number of planar sheets necessary to build up a compact isomer with an odd number of atoms is three, the next example is found for $n=16$, where the GS isomer is formed by the stacking of three $(\text{MgO})_5\text{Mg}^{2+}$ planar isomers. Similarly, the GS structures for $n=19$, 22, and 25 are stackings of three planar $(\text{MgO})_6\text{Mg}^{2+}$,

(MgO)₇Mg²⁺, and (MgO)₈Mg²⁺ isomers. All these isomers are specially compact for this reason. The next stacking of three planar isomers occurs for n=28, but the periodicity of three is not the only possible for these cluster sizes. The GS state of n=27 is formed by stacking five (MgO)₅Mg²⁺ planar isomers, and a new periodicity of five is expected to start at this cluster size (the GS structure for n=22 can be considered also as a stacking of five (MgO)₄Mg²⁺ planar sheets). For clusters larger than those studied in this work one would expect to see stackings of seven, nine, etc, planar structures. We will see in the next section that those periodicities are important to interpret the experimental abundance spectra.

A comparison with the results obtained for alkali halide cluster ions^{24,25} and neutral (MgO)_n clusters¹⁵ is illustrative. Hexagonal prismatic structures are very common for (MgO)_n clusters,¹⁵ as well as for some neutral alkali halide (AX)_n clusters.²¹⁻²³ However, rocksalt structures are clearly predominant for (MgO)_nMg²⁺ cluster ions, being this the main effect of nonstoichiometry and net charge: (a) perfect rocksalt structures can be built up with an odd number of ions (n=4,13,...), but an even number of ions is needed to construct a perfect hexagonal prism; (b) for “defect-like” structures, the extra charge is screened more effectively in the cuboid-like isomers. Examples can be found at n=3, where the hexagonal (MgO)₃ GS isomer¹⁵ converts into a rectangular structure upon adding Mg²⁺ to lower the repulsion between cations, and at n=10, where adding a triatomic Mg–O–Mg to the hexagonal prism which is the GS of the neutral (MgO)₉¹⁵ results in an isomer 0.57 eV less stable than that obtained by adding Mg–O–Mg to a rocksalt piece. Nevertheless, signs of the preference for hexagonal prismatic structures found in neutral (MgO)_n clusters can still be observed in the largest (MgO)_nMg²⁺ cluster ions. Specifically, (MgO)₉ and (MgO)₁₅ hexagonal subunits are observed for n=19, 25, and 27. Let us now compare with the results obtained for alkali halide cluster ions.^{24,25} While the GS isomers are not the same in many cases, overall the structures of (MgO)_nMg²⁺ cluster ions are similar to those obtained for (NaI)_nNa⁺ and (CsI)_nCs⁺.²⁵ There is just one major difference: centered hexagonal structures, containing an inner alkali cation with high coordination, were found frequently for (NaI)_nNa⁺ and (CsI)_nCs⁺, but such isomers are not observed for (MgO)_nMg²⁺. Evidently, the repulsion between oxide anions is larger than the repulsion between halide anions, and allocating six O²⁻ anions around a Mg²⁺ cation in energetically less favorable. In the next section we will see that this structural difference is important to understand the differences between the magic numbers observed in (MgO)_nMg²⁺ and in alkali halide cluster ions.

We finish this section with a discussion of the validity of pair potential models and the effects of the polarization correction on cluster structure. Comparison of our pair potential calculations with the aiPI results lead us to the following two important points: (a) pair potential models fail to reproduce quantitatively the expansion of the interionic distances with cluster size; (b) the energetical ordering of the different isomers for a given cluster

size is not reliable. On the positive side, the shape of the isomers is usually quite well reproduced, and the main structural correction obtained with an aiPI calculation is a global scaling of all the interionic distances. This last observation supports the use of pair potentials to locate good initial configurations for ionic clusters, from which *ab initio* calculations can be started. The effects of the polarization correction are rather negligible for n≥13. The main effect in that size range is a reduction of the energy differences between the isomers. The energetical ordering is affected only in those sizes showing near-degenerate isomers. An example is n=17, where an aiPI calculation without polarization predicts the second isomer in fig. 1 to be the GS. For n<13 the energy differences between isomers are smaller and the effects of polarization are more accussed. Specifically, linear chains are the GS isomers for n=1–3 and planar structures are the GS isomers for n=4–7 in aiPI calculations without polarization. Thus, inclusion of polarization speeds up the emergence of 3D structures.

B. Relative Stabilities. Comparison to Experimental Results.

In order to study the relative stabilities of (MgO)_nMg²⁺ cluster ions we calculate the evaporation threshold energy^{9,25} required to remove a MgO molecule from the ground state isomer. For a cluster (MgO)_nMg²⁺ this is done as follows: we consider the optimized GS structure and identify the MgO molecule that contributes the least to the cluster binding energy. Then we remove that molecule and relax the resulting (MgO)_{n-1}Mg²⁺ fragment to the nearest local minimum. The total energy required to evaporate a molecule is then the difference between the energy of the parent cluster and the energies of the two fragments, one of which is the MgO molecule:

$$E_{evaporation}(n) = E_{cluster}[(MgO)_{n-1}Mg^{2+}] + E(MgO) - E_{cluster}[(MgO)_nMg^{2+}]. \quad (7)$$

This process can be termed locally adiabatic because both fragments are allowed to relax to the local minimum energy configuration after the evaporation. For some cluster sizes, the fragment of size (n-1) left when a MgO molecule is removed from (MgO)_nMg²⁺ does not lie on the catchment basin of the (MgO)_{n-1}Mg²⁺ GS isomer, so that the evaporation threshold energies are larger than the energy differences between adjacent ground states minus E(MgO) in those cases. The evaporation energies are plotted as a function of n in figure 2. In the experiments performed by Ziemann and Castleman,¹⁶ the abundances in the mass spectra reflect the relative stabilities of (MgO)_nMg²⁺ cluster ions against evaporation of a MgO molecule. Starting from the largest cluster size studied, we can appreciate minima in figure 2 for n=28, 26, 23, 20, 17, 14, 12, 9, and 5. Thus, evaporation of a MgO molecule from those clusters is easy relative to evaporation from clusters of other sizes. Moreover, the curve shows abrupt increases precisely at those cluster sizes, so that evaporation of a MgO molecule from

the clusters of size $(n-1)$ is significantly more expensive than evaporation from cluster ions of size n . All of this results in an enrichment of $(\text{MgO})_n\text{Mg}^{2+}$ clusters with $n=4, 8, 11, 13, 16, 19, 22, 25,$ and 27 , a result which is in complete agreement with the experiment.¹⁶ Nevertheless, there is not a total correspondence between the experimental magic numbers and maxima in the evaporation energy curve. The experimental enhanced abundances result from a balance between two main processes: (a) evaporation from clusters with size $(n+1)$ results in an enrichment of the $(\text{MgO})_n\text{Mg}^{2+}$ clusters; (b) evaporation from clusters with size n has the opposite effect. A quantity that measures the stability of a $(\text{MgO})_n\text{Mg}^{2+}$ cluster ion relative both to $(\text{MgO})_{n+1}\text{Mg}^{2+}$ and $(\text{MgO})_{n-1}\text{Mg}^{2+}$ cluster ions is thus

$$\Delta_2(n) = E_{\text{evaporation}}(n+1) - E_{\text{evaporation}}(n), \quad (8)$$

where both terms in the difference are calculated using eq. (7) as explained above. This quantity is plotted as a function of n in Figure 3. Maxima are apparent at $n=4, 8, 11, 13, 16, 19, 22, 25,$ and 27 . Thus, the experimental results concerning enhanced relative stabilities are properly reproduced by our calculations.

As in the case of alkali halide clusters²³ and cluster ions,²⁵ the magic numbers observed for $(\text{MgO})_n\text{Mg}^{2+}$ can be explained in terms of a compactness argument. Most of those magic numbers are due to the occurrence of specially compact GS structures ($n=4, 13, 16, 22, 25,$ and 27). For the neighboring cluster sizes, the GS isomers have “defect-like” structures for which the Madelung interaction is optimized less effectively. $n=19$ has a “defect-like” GS structure which nevertheless is more compact than the GS structures of $n=18$ and $n=20$. The GS structures for $n=10$ and $n=12$ contain some low-coordinated ions that are not present in the $n=11$ GS isomer. Our explanation of the magic numbers and that offered by Ziemann and Castleman¹⁶ are essentially the same if we associate the formation of hexagonal subunits observed for some clusters in our work to the formation of terraces proposed by those authors (the only discrepancy is then the $n=11$ GS structure). The magic numbers show an striking periodicity of three from $n=13$ to $n=25$, that breaks first at $n=27$. These regular periodicities in the enhanced stabilities can be explained in terms of the structural trends described in the previous section. Specifically, for the size range studied in this work we can consider the planar isomers obtained for $n=4-8$ (some of which are not shown in Figure 1) as building blocks for the larger clusters. A stacking of at least three planar sheets is needed to build up a compact cluster with an odd number of ions, but it is also possible to stack 5, 7, 9, etc planar sheets. Starting from the stacking of three $(\text{MgO})_4\text{Mg}^{2+}$ planar isomers, this growing pattern explains all the magic numbers. $n=27$ breaks the periodicity of three because a more compact isomer is obtained stacking five $(\text{MgO})_5\text{Mg}^{2+}$ planar subunits than stacking three $(\text{MgO})_9\text{Mg}^{2+}$ planar subunits. Most of the magic numbers for $n \geq 30$ can be explained in this way. For example, stacking seven $(\text{MgO})_4\text{Mg}^{2+}$ planar isomers we would obtain a specially compact isomer for $n=31$; stacking five $(\text{MgO})_7\text{Mg}^{2+}$ planar isomers results in a compact

isomer for $n=37$, etc. These are magic numbers in the experiments.¹⁶ We conclude that the picture given in the work of Ziemann and Castleman¹⁶ for $n \geq 13$ is essentially correct and thus there is no need of more theoretical calculations to elucidate the structures of larger clusters.

Turning to the small-size regime, the magic numbers obtained for different alkali halide cluster ions^{6,25} are $n=4, 6, 9$ and 13 . The main magic numbers ($n=4$ and 13) are a consequence of the enhanced stability of very symmetrical rocksalt structures, and are observed also for $(\text{MgO})_n\text{Mg}^{2+}$ cluster ions. However, the “fine structure” peaks ($n=6, 9$ for alkali halide $(\text{AX})_n\text{A}^+$ cluster ions and $n=8, 11$ for $(\text{MgO})_n\text{Mg}^{2+}$) differ. Specially compact structures can be formed for $(\text{AX})_6\text{A}^+$ and $(\text{AX})_9\text{A}^+$, namely centered hexagonal configurations, resulting in an enhanced stability for those cluster sizes.²⁵ But those structures are not even low-lying isomers for $(\text{MgO})_n\text{Mg}^{2+}$, and the clusters formed for $n=9$ and $n=12$ are not specially compact. Thus, the explanation of the magic numbers is the same in both cases. The structural differences between both materials determine which are the specific magic numbers.

IV. SUMMARY

The *ab initio* perturbed ion model, supplemented with a semiempirical treatment of dipolar terms, has been employed in order to study the structural and energetic properties of $(\text{MgO})_n\text{Mg}^{2+}$ ($n=1-29$) cluster ions. We have used a rigid ion model to generate a large set of initial configurations for each cluster size. Next, those structures have been optimized without consider any equivalence between different ions, allowing thus for an appropriate geometrical relaxation. Correlation corrections, which turned out to be essential for a proper description of $(\text{MgO})_n$ clusters,¹⁵ have been added to the Hartree-Fock energies for all cluster sizes. Inclusion of polarization corrections at a semiempirical level reduces a little the reliability of the model compared to full *ab initio* methods, but allows to perform such a systematic study with appropriate geometrical relaxations at a significantly reduced computational cost. The structural trends of $(\text{MgO})_n\text{Mg}^{2+}$ cluster ions have been described. The emergence of the bulk crystalline symmetry proceeds in different overlapping stages, from one-dimensional configurations for $n=1-3$ to planar structures for $n=3-8$, and then to three-dimensional structures with a clear predominance of rocksalt structures from $n=13$ on. For $(\text{MgO})_{13}\text{Mg}^{2+}$, a perfect $3 \times 3 \times 3$ rocksalt isomer appears which serves as a building block for larger cluster ions. Specially compact isomers can be built up by stacking an odd number of the planar isomers found in the size range $n=3-8$. A comparison with the structures obtained for neutral $(\text{MgO})_n$ clusters¹⁵ shows that the preference for cuboid-like structures is a direct consequence of nonstoichiometry and net charge. Comparison with the structures obtained for alkali halide cluster ions²⁵ reveals some differences that can be explained in terms of the larger repulsion between oxide anions compared to the repulsion between halide anions. The main

effect of the polarization correction is to speed up the emergence of 3D structures. Once those 3D structures are well established polarization plays just a minor role.

The relative stabilities of $(\text{MgO})_n\text{Mg}^{2+}$ cluster ions have been studied by calculating the energy required to evaporate a MgO molecule from the GS structures and the first differences between those evaporation energies, that reflect the stability of a cluster of size n relative to the stabilities of the neighbor clusters of sizes $(n+1)$ and $(n-1)$. Both sets of calculations predict the clusters with $n=4, 8, 11, 13, 16, 19, 22, 25,$ and 27 to be specially stable, a result that is in complete agreement with the experimental enhanced abundances reported by Ziemann and Castleman.¹⁶ Those enhanced stabilities have been explained in terms of a compactness argument, namely it is possible to construct isomers for those values of n that are more compact than for the neighboring sizes.

Finally, a comparison has been made with the results obtained by using a phenomenological pair potential model. This comparison has shown that, while pair potential calculations are really helpful when obtaining initial guesses for the isomer geometries, the distances and the energetical ordering of the isomers obtained with them are generally not reliable.

The authors gratefully acknowledge Prof. J. D. Gale for providing us with a copy of reference 37 and Prof. A. W. Castleman Jr. for discussing with us the experimental results in reference 16. Work supported by DGES (PB95-0720-C02-01) and Junta de Castilla y León (VA63/96). A. Aguado is supported by a predoctoral fellowship from Junta de Castilla y León.

Captions of figures

Figure 1. Lowest-energy structure and low-lying isomers of $(\text{MgO})_n\text{Mg}^{2+}$ cluster ions. Light balls are Mg^{2+} cations and dark balls are O^{2-} anions. The energy difference (in eV) with respect to the most stable structure is given below the corresponding isomers. For $n \geq 24$ only the ground state isomer is shown.

Figure 2. Evaporation threshold energies required to remove a neutral MgO molecule from $(\text{MgO})_n\text{Mg}^{2+}$ cluster ions as a function of n .

Figure 3. Second derivative $\Delta_2(n)$ for $(\text{MgO})_n\text{Mg}^{2+}$ cluster ions as a function of the cluster size. Maxima identify those cluster sizes with an enhanced relative stability.

* Corresponding Author.

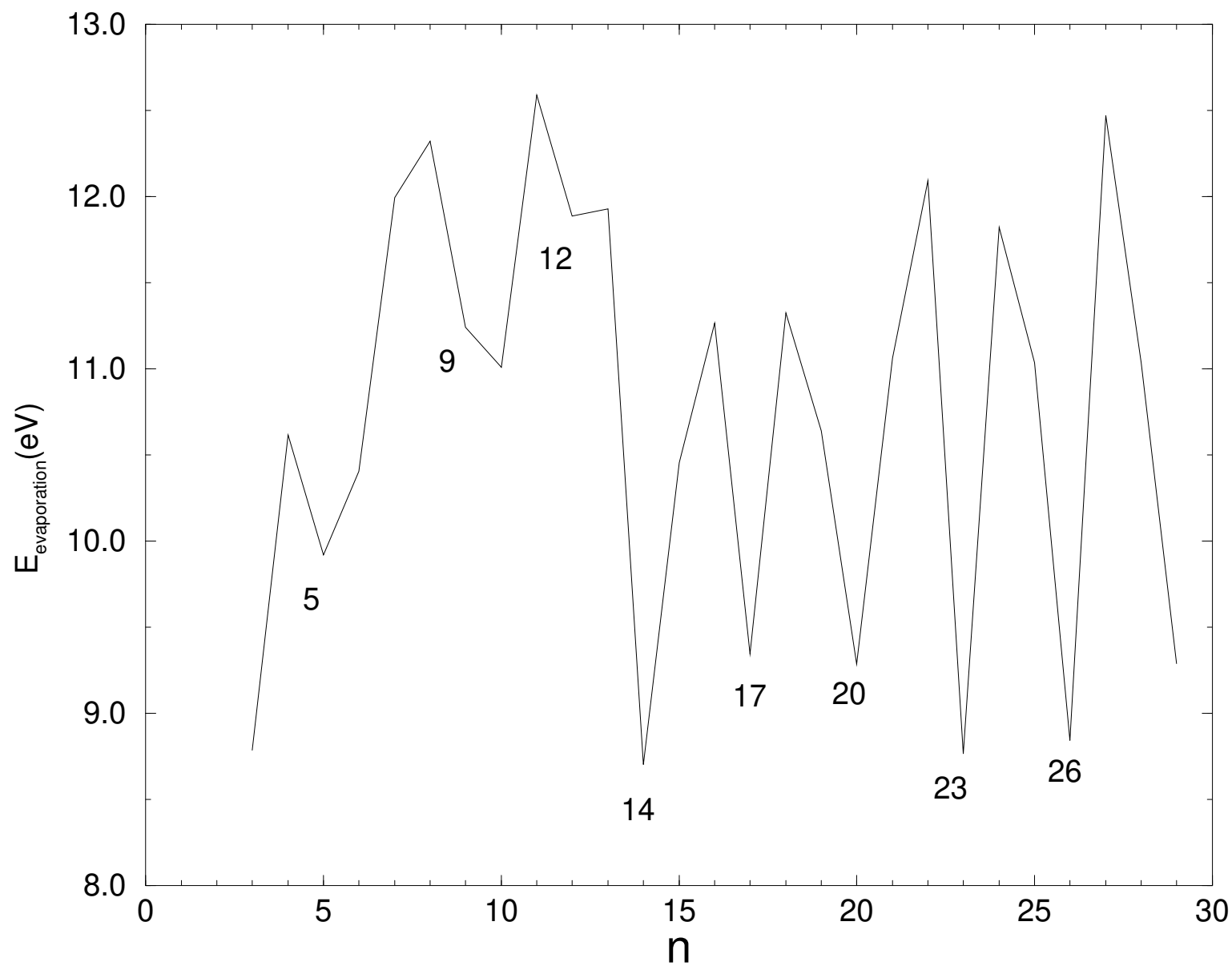
¹ W. A. Saunders, *Phys. Rev. B* **37**, 6583 (1988).

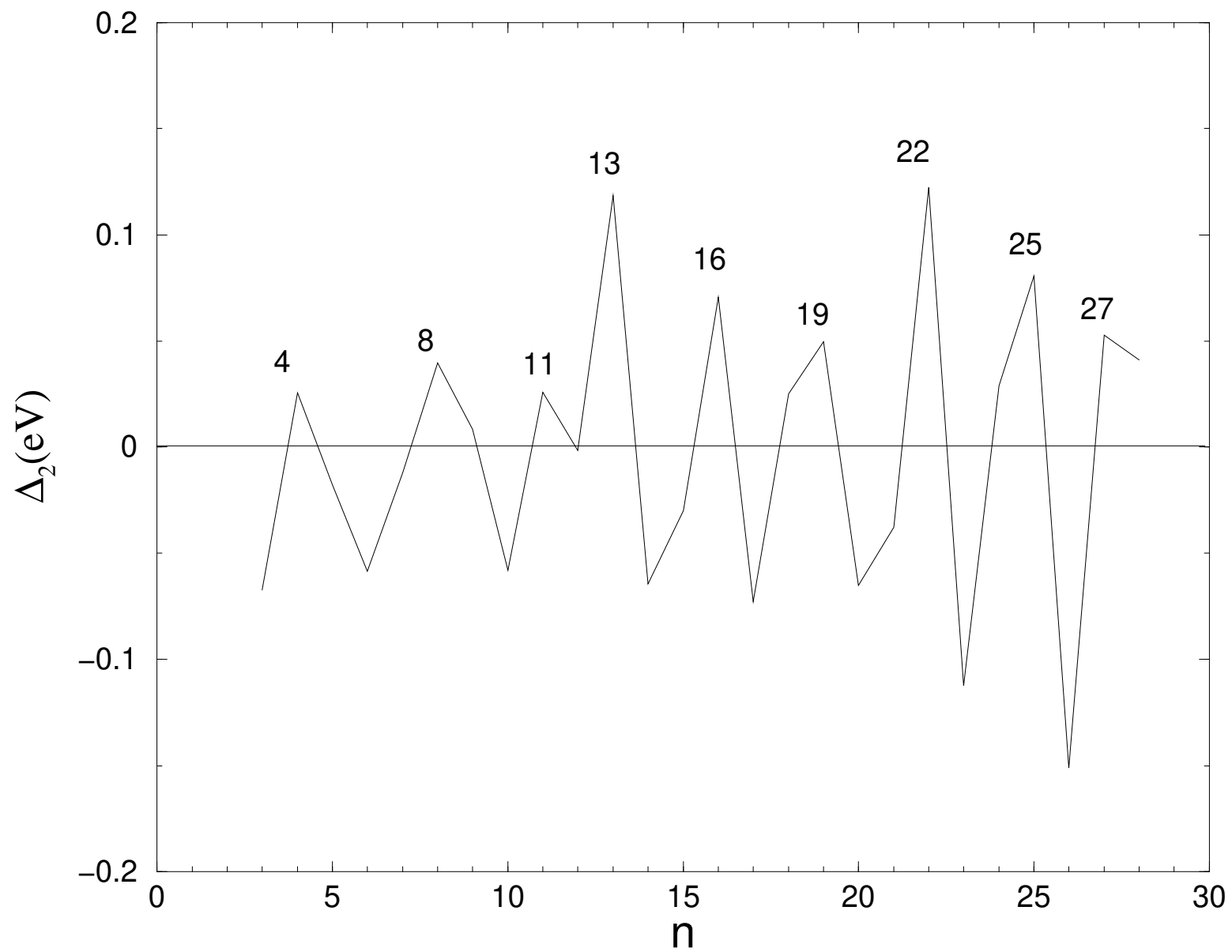
² W. A. Saunders, *Z. Phys. D* **12**, 601 (1989).

³ P. J. Ziemann and A. W. Castleman, Jr., *Z. Phys. D* **20**, 97 (1991).

- ⁴ P. J. Ziemann and A. W. Castleman, Jr., *J. Chem. Phys.* **94**, 718 (1991).
- ⁵ C. W. S. Conover, Y. A. Yang, and L. A. Bloomfield, *Phys. Rev. B* **38**, 3517 (1988).
- ⁶ Y. T. Twu, C. W. S. Conover, Y. A. Yang, and L. Bloomfield, *Phys. Rev. B* **42**, 5306 (1990).
- ⁷ T. P. Martin, *Phys. Rep.* **95**, 168 (1983).
- ⁸ J. Diefenbach and T. P. Martin, *Surf. Sci.* **156**, 234 (1984).
- ⁹ N. G. Phillips, C. W. S. Conover, and L. A. Bloomfield, *J. Chem. Phys.* **94**, 7498 (1991).
- ¹⁰ S. Moukouri and C. Noguera, *Z. Phys. D* **24**, 71 (1992).
- ¹¹ S. Moukouri and C. Noguera, *Z. Phys. D* **27**, 79 (1993).
- ¹² J. M. Recio and R. Pandey, *Phys. Rev. A* **47**, 2075 (1993).
- ¹³ J. M. Recio, R. Pandey, A. Ayuela, and A. B. Kunz, *J. Chem. Phys.* **98**, 4783 (1993).
- ¹⁴ M. J. Malliavin and C. Coudray, *J. Chem. Phys.* **106**, 2323 (1997).
- ¹⁵ E. de la Puente, A. Aguado, A. Ayuela, and J. M. López, *Phys. Rev. B* **56**, 7607 (1997).
- ¹⁶ P. J. Ziemann and A. W. Castleman, Jr., *Phys. Rev. B* **44**, 6488 (1991).
- ¹⁷ V. Luaña and L. Pueyo, *Phys. Rev. B* **41**, 3800 (1990).
- ¹⁸ S. Huzinaga and A. A. Cantu, *J. Chem. Phys.* **55**, 5543 (1971).
- ¹⁹ S. Huzinaga, D. McWilliams, and A. A. Cantu, *Adv. Quantum Chem.* **7**, 183 (1973).
- ²⁰ S. Huzinaga, L. Seijo, Z. Barandiarán, and M. Klobukowski, *J. Chem. Phys.* **86**, 2132 (1987).
- ²¹ A. Ayuela, J. M. López, J. A. Alonso, and V. Luaña, [a] *Z. Phys. D* **26**, S213 (1993); [b] *An. Fis. (Spain)* **90**, 190 (1994); [c] *Physica B* **212**, 329 (1996).
- ²² A. Aguado, A. Ayuela, J. M. López, and J. A. Alonso, *J. Phys. Chem. B* **101**, 5944 (1997).
- ²³ A. Aguado, A. Ayuela, J. M. López, and J. A. Alonso, *Phys. Rev. B* **56**, 15353 (1997).
- ²⁴ A. Ayuela, J. M. López, J. A. Alonso, and V. Luaña, *Can. J. Phys.* **76**, 311 (1998).
- ²⁵ A. Aguado, A. Ayuela, J. M. López, and J. A. Alonso, *Phys. Rev. B*, accepted.
- ²⁶ V. Luaña, J. M. Recio, and L. Pueyo, *Phys. Rev. B* **42**, 1791 (1990).
- ²⁷ G. von Helden, M. T. Hsu, P. R. Kemper, and M. T. Bowers, *J. Chem. Phys.* **95**, 3835 (1991).
- ²⁸ M. F. Jarrold, *J. Phys. Chem.* **99**, 11 (1995).
- ²⁹ M. Maier-Borst, P. Löffler, J. Petry, and D. Kreisle, *Z. Phys. D* **40**, 476 (1997).
- ³⁰ V. Luaña, M. Flórez, E. Francisco, A. Martín Pendás, J. M. Recio, M. Bermejo, and L. Pueyo, in *Cluster Models for Surface and Bulk Phenomena*, edited by G. Pacchioni, P. S. Bagus and F. Parmigiani (Plenum, New York, 1992), p. 605.
- ³¹ R. McWeeny, *Methods of molecular quantum mechanics*, Academic Press. London (1994).
- ³² E. Francisco, A. Martín Pendás, and W. H. Adams, *J. Chem. Phys.* **97**, 6504 (1992).
- ³³ E. Clementi, *IBM J. Res. Develop.* **9**, 2 (1965).
- ³⁴ S. J. Chakravorty and E. Clementi, *Phys. Rev. A* **39**, 2290 (1989).
- ³⁵ V. Luaña, A. Martín Pendás, J. M. Recio, and E. Francisco, *Comput. Phys. Commun.* **77**, 107 (1993).
- ³⁶ E. Clementi and C. Roetti, *At. Data and Nuc. Data Tables* **14**, 177 (1974).
- ³⁷ T. S. Bush, J. D. Gale, C. R. A. Catlow, and P. D. Battle, *J. Mater. Chem.* **4**, 831 (1994).

- ³⁸ J. A. Nelder and R. Mead, *Comput. J.* **7**, 308 (1965).
- ³⁹ W. H. Press and S. A. Teukolsky, *Computers in Physics* **5**, 426 (1991).
- ⁴⁰ P. W. Fowler and N. C. Pyper, *Proc. R. Soc. Lond. A* **398**, 377 (1985).
- ⁴¹ R. F. W. Bader, *Atoms in Molecules* (Oxford University Press, Oxford, 1990).
- ⁴² A. Martín Pendás, A. Costales, and V. Luaña, *Phys. Rev. B* **55**, 4275 (1997).
- ⁴³ M. Matsui, *J. Chem. Phys.* **108**, 3304 (1998).





This figure "aguado.fig1.mgomg2+.gif" is available in "gif" format from:

<http://arxiv.org/ps/physics/9808036v1>

This figure "aguado.fig1cont.mgomg2+.gif" is available in "gif" format from:

<http://arxiv.org/ps/physics/9808036v1>

This figure "aguado.fig1contt.mgomg2+.gif" is available in "gif" format from:

<http://arxiv.org/ps/physics/9808036v1>

This figure "aguado.fig1conttt.mgomg2+.gif" is available in "gif" format from:

<http://arxiv.org/ps/physics/9808036v1>

This figure "aguado.fig1contttt.mgomg2+.gif" is available in "gif" format from:

<http://arxiv.org/ps/physics/9808036v1>

This figure "aguado.fig1conttttt.mgomg2+.gif" is available in "gif" format from:

<http://arxiv.org/ps/physics/9808036v1>